LANGMUIR Article
Cite This: Langmuir 2019, 35, 12009−12016
pubs.acs.org/Langmuir

Electrochemical Study of Structure Tunable Perylene Diimides and The Nanofibers Deposited on Electrodes

Zexu Xue,[†] Shuai Chen,*[,†,‡] Yu Xue,[†] Olivia Anielle Watson,[‡] and Ling Zang*[,‡]

[†]School of Pharmacy, Jiangxi Science & Technology Normal University, Nanchang 330013, Jiangxi China

[‡]Nano Institute of Utah and Department of Materials Science and Engineering, University of Utah, Salt Lake City 84112, Utah United States

Supporting Information

ABSTRACT: The electrochemical behavior of organic conjugated semiconductors and their bulk materials is a considerable and irreplaceable parameter to maintain their diverse electronic or optoelectronic applications. In this paper, a series of n-type symmetrical perylene diimide derivatives (PTCDIs) with substituents (3,4-ethylenedioxythiophene (EDOT), cyclohexane, acetic acid, or propionic acid) at located the nitrogens imide position were synthesized, and their solubility, optical features, thermal stability, as well as solution-phase interfacial self-assembly into one-dimensional (1D) nanofibers and related morphology were discussed in detail. Moreover, a simple but effective method, in situ deposition following in situ self-assembly, was developed to construct uniform electrodes over a large area coated with networked PTCDI nanofibers. Then the electrochemical properties of the PTCDI nanofibers were researched in comparison with their molecules. The excellent variability at molecular or nanoscale morphological level will provide an interesting insight into the research of PTCDIs in a wide range applications of organic electronics.

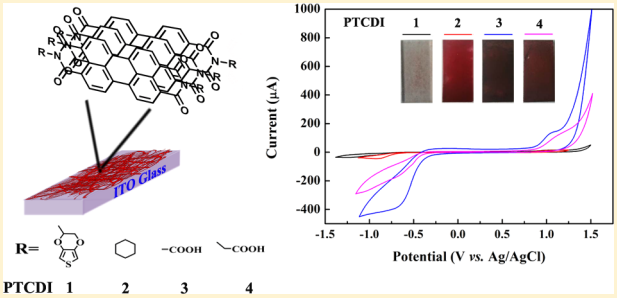

INTRODUCTION

Organic π-conjugated semiconductors, including small molecules, conducting polymers, and their assemblies, have been intensively reported in the fields of organic electronics such as organic photovoltaic devices (OPVs), organic field effect transistors (OFETs), organic light emitting diodes (OLEDs), electrochromic devices (ECs), sensors, and so on.[1−6] For these advanced systems, the energy levels of frontier molecular orbitals play a crucial role in controlling the sequential charge carrier transport crossing the heterojunction interfaces, which in turn determine the overall device efficiency. Electrochemical measurements provide effective ways for characterizing the electronic structure of molecular materials, particularly the energy levels of molecular orbitals and the related surface redox potentials. Systematic analysis and comparison of these parameters would help to improve and to optimize the electronic and optoelectronic performance of new materials developed in the next generation.

The above-mentioned electrochemistry study has been widely utilized in conductive polymers like well-known poly(3,4-ethylenedioxythiophene) (PEDOT) and the related devices. Most of the polymers display p-type behavior, for which positive holes act as the main charge carriers, and possess highly conjugated structure in planar skeleton.[7−9] Some other polymers structure containing electron donor and acceptor units, thus forming D−A configuration, have been proven to be capable of increasing the carrier mobility. Nonetheless, far fewer n-type materials have been developed for research and device development than for many p-type materials. Electronic systems usually require both n- and p-type materials which are complementary in forming p−n junctions. However, it is a main challenge to develop n-type materials from conjugated molecules based on the air stability, thus, the absorbed oxygen on material surface often acts the competitive electron acceptor, while depleting the electrons, which are the major charge carriers of n-type materials.

Molecules based on perylene-3,4,9,10-tetracarboxylic diimides (PTCDIs) can assemble (mainly through the π−π stacking interaction) and form a unique class of n-type materials with strong thermal stability and high fluorescence quantum yield; a combination which enables a wide range of applications in electronic and optoelectronic fields.[10−14] In particular, the large, rigid, planar conjugation structure of PTCDIs is highly conducive to the one-dimensional (1D) cofacial stacking, which leads to the formation of nanofiber structures.[10] In the past decade, our group has been working extensively on the design and synthesis of various structures of PTCDIs, as well as their self-assembly and optoelectronic properties.[10,14] Since the two imide positions are nodes in the π-orbitals of PTCDI, the substitution at the imide position does not observably change the molecular electronic structure, including the band gap. This offers enormous options to adjust

Received: June 25, 2019
Revised: August 12, 2019
Published: August 21, 2019

DOI: 10.1021/acs.langmuir.9b01943
Langmuir 2019, 35, 12009−12016

the side-chain structure of PTCDI (while maintaining the basic electronic property) so as to control and optimize the intermolecular stacking, and the morphology and crystalline structure of self-assembled nanofibers.[11−13] One unique feature of the nanofiber structure is the increased charge transport along the long axis mediated by the effective intermolecular electron delocalization.[15] Through extensive investigations in past years, our lab has developed comprehensive protocols for the solution-phase self-assembly that can lead to the formation of shape-defined structures, for which the key parameters include selection of solvent, temperature, and concentration.[10,14] It is important to select a fitted solution to form PTCDIs nanofibers, which is finally determined by the balance between the solubility of PTCDIs molecules and noncovalent intermolecular forces, in conjunction with proper molecular design.[10] The solution-phase self-assembly process and condition, which is based on a mass transfer process between good and poor solvent, should be optimized by adjusting solution components. A good solvent for PTCDIs has a high degree of solubility and generally is a polar aprotic solvent like $CHCl_3$, whereas PTCDIs have limited solubility in the poor solvent like CH_3OH which is favorable for $\pi-\pi$ stacking.

Although PTCDIs have been extensively used as electronic and optoelectronic materials in a broad range of devices such as OPVs, OFETs, OLEDs, and sensors, the electrochemistry of PTCDIs (especially the nanofibers) is much less studied.[10,13−18] One technical challenge for the nanofibers study is how to deposit the nanofibers onto the electrode surface to form a homogeneous and compact thin layer covering the whole electrode to achieve measurement with high peak currents. If successful, the electrochemical measurement of PTCDI nanostructures would provide new information for how to design high-performance semiconductor materials in relation to the tunable electrical properties. Comparison of the electrochemical observations of PTCDI molecules and assemblies could provide a deeper insight into the structure−property relationship regarding the intermolecular arrangement, and the effect on the charge transport.

In previous work, we have demonstrated symmetric PTCDIs were substituted with dodecyl chains at both sides to be capable of formation of nanofibers with crystalline structures, and can be characterized with electrochemistry.[14] Following this, here, we will study five PTCDIs specially designed with different side substitutions, aiming to investigate the structural dependence of the electrochemical properties. As shown in Figure 1, the symmetric four PTCDIs were substituted by EDOT, cyclohexane, acetic acid, and propionic acid, respectively, while one asymmetrical PTCDI 5 owning both dodecyl and EDOT as terminal groups (shown in Scheme S1)

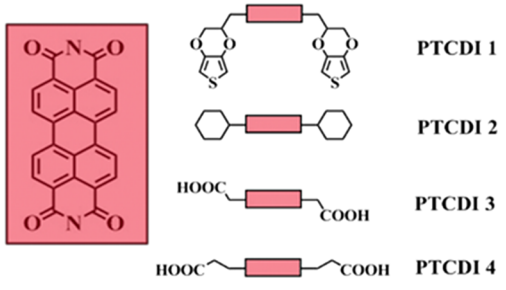

Figure 1. Molecular structures of PTCDIs synthesized in this work all for electrochemistry study at both molecular and assembly state.

was introduced for comparison. As one of the most popular conjugated electron-donors, EDOT possesses interesting electrochemical properties and can be easily oxidized into polymeric powders or films, which can be used as p-type semiconductors and/or conductive coatings in different organic electronic systems. However, the bisubstitution of EDOT significantly reduces the solubility of PTCDI 1 molecule in organic solvents. To improve the solubility, PTCDI 5 and PTCDI 2 (two sides substituted with cyclohexane) were synthesized, and both molecules were also favorable for 1D self-assembly, forming shape-defined nanofiber structure, via the bisolvent interfacial phase-transfer method.[10] PTCDI 3 substituted with acetic acid was found soluble in aqueous solution, whereas PTCDI 4 substituted with propionic acid had increased solubility in organic solvents.[18,19] The selected five molecules provide a variety of solubility and self-assembly properties, offering great opportunities for us to investigate the electrochemical behavior both in the solution phase and on the electrode surface. Particularly, we developed in this study a unique way to deposit high quality, uniform nanofiber on ITO electrodes. Moreover, the reliable electrical property, and more importantly, the correlation of the measurement with the UV−vis absorption and fluorescence optical properties were measured and discussed.

EXPERIMENTAL SECTION

Molecular Synthesis and Characterization. Details of the synthesis of five PTCDI 1−5 are described in the Supporting Information (SI) with the synthesis pathways shown in Scheme S1. Generally, substitution at the imide position is realized through a one-step reaction between the anhydride precursor of PTCDI and the primary amine moiety of a target side-chain group. The reaction is highly thermodynamic favorable, usually in high yield. The five molecular structures prepared were characterized by NMR and FT-IR spectra as shown in SI Figure S1. All PTCDIs showed excellent thermal stability as evidenced by the thermogravimetric analysis (TGA) with results shown in SI Figure S2. Two of the five molecules, PTCDI 1 and 2, exhibited the strongest thermal stability, with transition temperatures above 400 °C, likely due to the strong intermolecular stacking.[10] Certain degree of solubility of the PTCDIs is required for solution processing of the molecular self-assembly, and the related spectroscopy and electrochemistry experiments. The solubility results of PTCDIs and related discussion are displayed in SI Table S1. Materials characterization is listed in the Supporting Information in detail.

Fabrication of PTCDIs Nanofibers. The PTCDIs nanofibers were fabricated by the molecular self-assembly induced at the interface between a good and poor solvent, which was previously developed in our lab.[10] The experimental details can be found in the SI. The 1D self-assembly (or the length-to-width ratio of nanofibers) is strongly affected by the steric hindrance caused by the side groups. In general, the smaller the side groups, the longer and thinner fibers will be formed. On the other hand, side groups possessing more conjugated structures often result in a decreased solubility of the molecules, making it difficult for solution processing of the self-assembly. Due to this trade off, a medium size side group is usually favorable for self-assembly of PTCDIs. All the selected candidate molecules in this work possess side groups in medium size.

RESULTS AND DISCUSSION

UV−Vis and Fluorescence Spectroscopy of PTCDIs. Figure 2 and SI Figure S3 show the UV−vis absorption of PTCDIs at the increasing concentrations of 5, 10, 15, 20, and 25 μmol L^{-1}. PTCDI 1 and PTCDI 2 display similar absorption spectra, with three characteristic peaks located around at 460, 490, and 528 nm due to the $\pi-\pi^*$ electronic

DOI: 10.1021/acs.langmuir.9b01943
Langmuir 2019, 35, 12009−12016

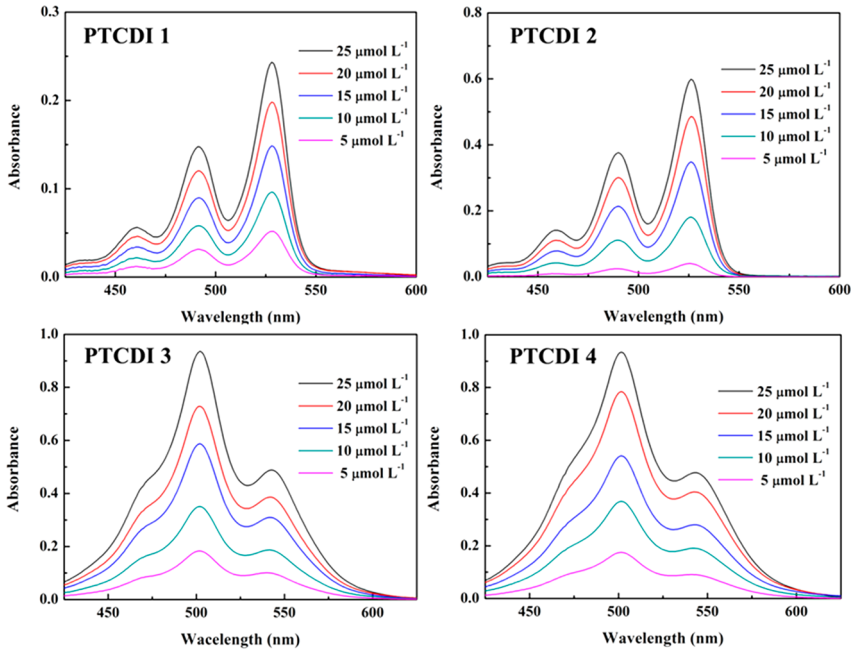

Figure 2. UV−vis absorption spectra of PTCDI 1 and PTCDI 2 (in $CHCl_3$), and PTCDI 3 and PTCDI 4 (in aqueous solution containing 6 M of triethylamine), at increasing concentrations as marked in the figure.

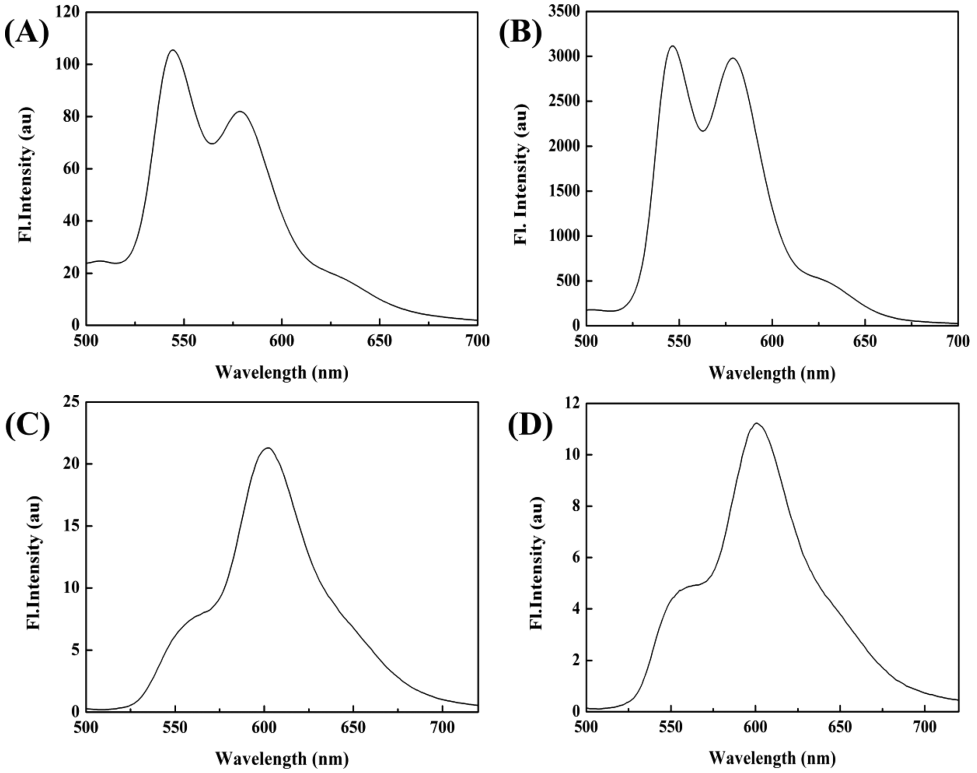

Figure 3. Fluorescent spectra of (A) PTCDI 1, (B) PTCDI 2, (C) PTCDI 3, (D) PTCDI 4. The concentrations of all PTCDIs are under saturation states.

transitions, corresponding to 0 → 2, 0 → 1, and 0 → 0 electronic vibration, respectively.[20] In comparison, different absorption features are observed for PTCDI 3 and PTCDI 4, for which the 0 → 1 transition becomes more dominant than the 0 → 0 transition, in reverse to the common observation of PTCDIs dissolved in organic solvents. The dominant 0 → 1 absorption peak usually indicates dimeric stacking of the PTCDIs, which in this case is likely caused by the ion pair structure.[18] Under high concentrations of triethylamine (6 M) in an aqueous solution, PTCDI 3 and PTCDI 4 are completely deprotonated, forming the acetate ion ($-COO^-$). Acetate anions and triethylamine cations thus formed are favorable for the formation of ion pairs stabilized in water, which in turn may facilitate the dimeric stacking of PTCDIs.[18]

DOI: 10.1021/acs.langmuir.9b01943
Langmuir 2019, 35, 12009−12016

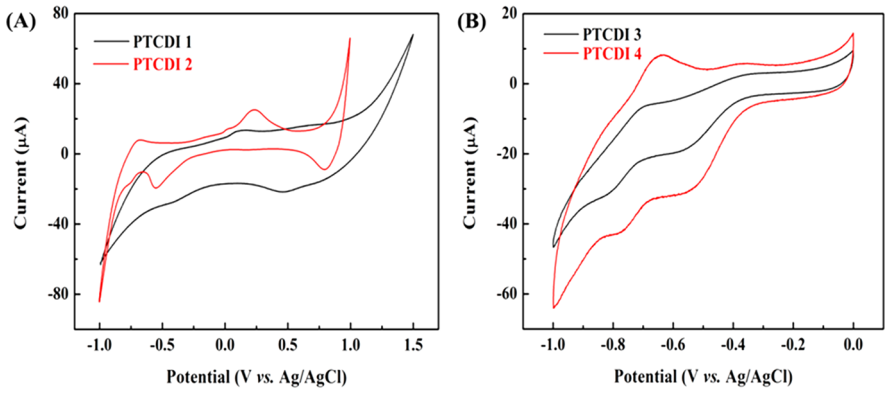

Figure 4. Cyclic voltammograms of (A) PTCDI 1 and PTCDI 2 in $CHCl_3/Bu_4NPF_6$ (0.1 M) with saturated concentration at 25 °C, (B) PTCDI 3 and PTCDI 4 in distilled water/Na_2SO_4 (0.1 M) with 0.1×10^{-3} M at 25 °C. The scan rate was 100 mV/s and Pt wire was as the working electrode and the counter electrode, while Ag/AgCl was as the reference electrode.

Fluorescent emission behaviors of PTCDIs are intuitively observed in Figure 3 and SI Figure S4. Three characteristic emission peaks of PTCDI 1, PTCDI 2, and PTCDI 5 were located near 546, 579, and 630 nm, respectively. The fluorescence intensities are largely derived from their different molecular saturated concentration in $CHCl_3$. An interesting phenomenon was observed for PTCDI 3 and PTCDI 4, that is when adding isopyknic methanol in aqueous solutions, they could display intensive fluorescence light as shown in SI Figure S4(B) due to the addition of organic hydrosoluble solvents quickly changing the pH value and varying the solution system. Moreover, PTCDIs assembly could be tested from the absorption spectra at long wavelength ranges as seen in SI Figure S5. One major explanation is that the H-type aggregations of PTCDIs decrease the intensity of characteristic absorption peaks of 0 → 1 and 0 → 0 vibronic bands.[21,22] In addition, with the end of self-assembly for PTCDIs, the accompanying reduction of fluorescence intensity could be explained by the effect of aggregation-caused quenching (ACQ).

Electrochemistry of Molecular PTCDIs. Molecular electrochemical properties of PTCDI 1−4 are illustrated in Figure 4, and those of PTCDI 5 are seen in SI Figure S6. When scanning cathodically from 0 to −1 V, every sample exhibited first reduction peak around −0.5 V, indicating the electron-deficient feature of PTCDI core. Due to the introduction of electron-donating EDOT unit into PTCDI at the imide position, PTCDI 1 and PTCDI 5 exhibited the onset initial oxidation potential at 1.0 V in the anodic range, which corresponds with EDOT's initial oxidation potential. However, it should be emphasized that the diversity of the substituents at imide positions has little effect on the redox potentials; even replacing cyclohexane by electron-donating EDOT groups increased the onset initial oxidation potential by only 0.13 V. Apparent nodes at the nitrogens imide has a negligible influence on the optical and electrochemical properties of PTCDIs. However, PTCDI 3 and PTCDI 4 showed two reduction peaks at the range of 0 to −1 V, which are −0.5 V and −0.8 V, respectively. The former potential represents one-electron reduction of PTCDI to the monoanionic ($PTCDI^-$), whereas the latter potential arises from a reduction of triethylamine molecule. The limited numbers of fully soluble PTCDI 3 and PTCDI 4 in neutral aqueous environment or organic solvents affect their redox properties due to the inferior hydrogen bond interaction of PTCDIs.[21] All cyclic voltammetry (CV) curves of the PTCDIs show one quasi-reversible reduction process in voltammograms, arising from the carbonyl oxygen of PTCDIs core skeleton, which consists with the n-type behavior property of PTCDIs. As shown in Table 1, for PTCDI 3 and PTCDI 4, both the HOMO and LUMO energy levels decrease than that of other PTCDIs. This phenomenon can be assumed to the better ability of COO^- to lose electrons than other substituents. Moreover, due to the limited solubility of all PTCDIs in organic solvent, the first reduction process of PTCDIs removes the delocalizing of the surplus electron density.

Table 1. Optical and Electrochemical Properties of PTCDI 1-4

PTCDIs	HOMO/ eV	LUMO/ eV	E_{ox}^{onset}/V	λ_{abs}/nm	λ_{emi}/ nm	E_g/ eV[b]
1[a]	−5.92	−3.67	1.12	460, 491, 528	544, 582	2.25
2[a]	−5.62	−3.36	0.82	459, 490, 526	546, 578	2.26
3[c]	−6.60	−4.11		501, 542	557, 589	2.12
4[c]	−6.63	−4.13		501, 543	558, 590	2.12

[a]HOMO and LUMO levels are calculated using the formula HOMO= $-(E_{ox}^{onset} + 4.8)$ eV; LUMO= (HOMO + E_g) eV. [b]Estimated values from the UV−vis absorption edge of the PTCDIs solution (E_g = 1240/ λ_{abs}eV) [c]The LUMO and HOMO of PTCDI 3 and PTCDI 4 were evaluated from Gaussian theoretical simulation based on B3LYP/6-31G.

The relationship between electrochemistry and molecules has attracted many interpretations from solubility, steric hindrance, types of electrodes, and so on. In view of the poor solubility and inherent steric hindrance of PTCDI 1 molecule, and nonconjugated junction between PTCDI core and EDOT unit, their electropolymerization on utilized electrodes and electrolytes were a failure in contrast to many studies of EDOT. Thus, research about the electrochemical activities of molecular assemblies of PTCDIs will be of great help for t optoelectronic applications.

Morphologies of Nanofibers PTCDIs via Self-Assembly. Our group's previous work made a huge effort toward outstanding optoelectrical properties of PTCDIs in optoelectronics springing from the defect-free and well-ordered molecular packing enabled by strong intermolecular π−π

DOI: 10.1021/acs.langmuir.9b01943
Langmuir 2019, 35, 12009−12016

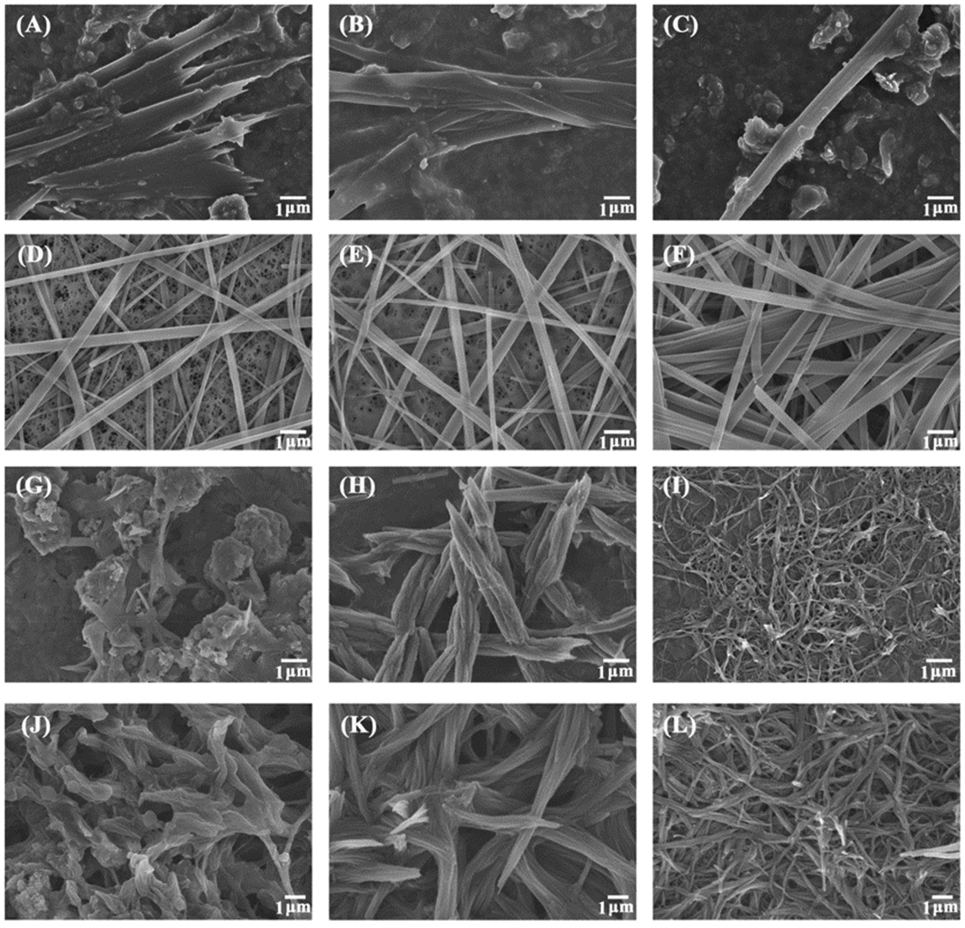

Figure 5. SEM images of PTCDI 1 (A–C), PTCDI 2 (D–F), PTCDI 3 (G–I), and PTCDI 4 (J–L) nanofibers self-assembled in three solvent systems with V_{good}:V_{poor} = 1:1, 1:2, 1:4 under 25 °C.

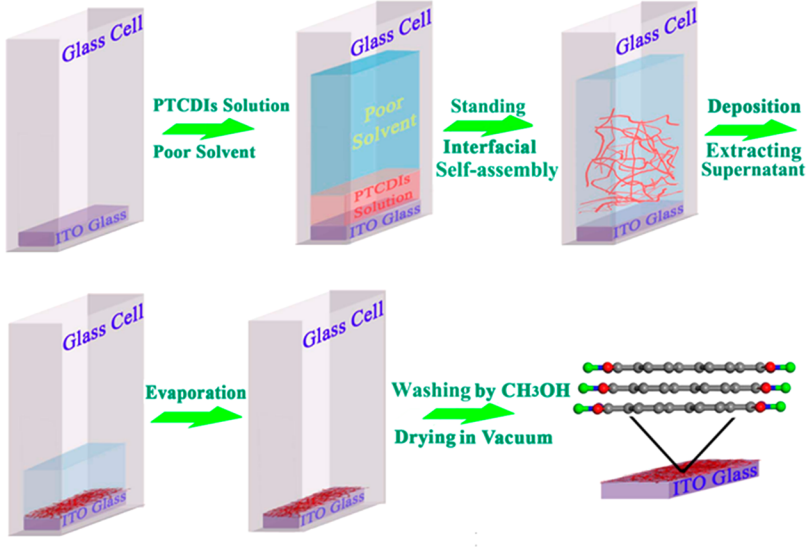

Figure 6. Schematic image of fabricating PTCDIs nanofibers coated ITO electrode via in situ interfacial self-assembly and in situ deposition at room condition.

interactions.[10,14] So herein, we employed the relying interfacial self-assembly method to fabricate PTCDI nanofibers as the morphology images shown in Figure 5 and SI Figures S7 and S8. When increasing the poor solvent in a blending solvent system, the nanosized morphologies were predominantly optimized under V_{good}:V_{poor} = 1:1 to 1:4, where the aspect ratios of all PTCDIs were sequentially increased together with much uniform features. In contrast, PTCDI 2 nanofibers exhibited much regular and smooth morphology than PTCDI 1 due to the slight size of cyclohexane than EDOT. Due to the

DOI: 10.1021/acs.langmuir.9b01943
Langmuir 2019, 35, 12009–12016

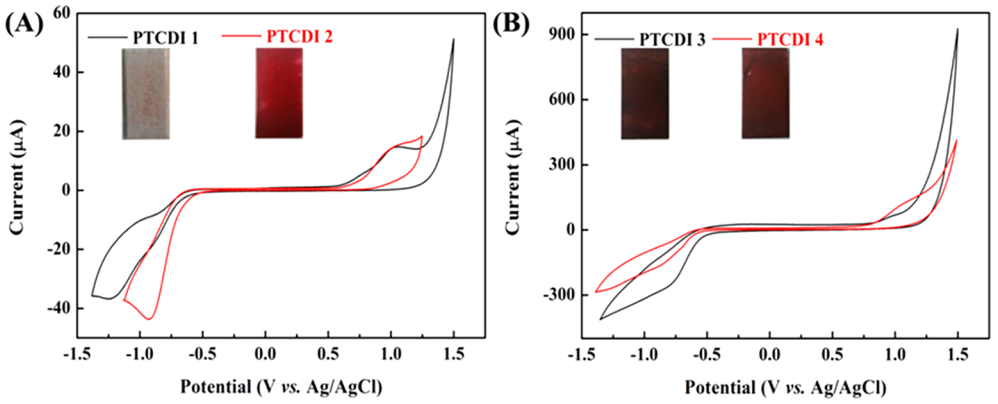

Figure 7. Cyclic voltammograms of (A) PTCDI 1 and PTCDI 2, (B) PTCDI 3 and PTCDI 4 nanofibers in 0.1 M Na_2SO_4 aqueous solution at 25 °C, under the scan rate of 100 mV/s, with ITO glass as the working electrode, Pt disk as the counter electrode, and Ag/AgCl as the reference electrode.

presence of COOH unit, PTCDI 3 and PTCDI 4 are sensitive to pH lead to protonation and deprotonation of COOH. Thus, under V_{good}:V_{poor} = 1:4, PTCDI 3 and PTCDI 4 showed similar 1D nanofibril morphology.

Fabrication of Uniform Electrodes Covering Nanofibers PTCDIs. Up to now, scarce studies have focused not only on the electrochemistry research of PTCDIs but also overcoming the restriction of covering their nanoscale assemblies onto the electrode surfaces. The most investigated method of coating PTCDI molecules on electrodes was vapor-deposition on electrodes, while we previously transported PTCDI nanofibers from self-assembled solutions onto Gold electrodes via the sucking-dripping way.[14] However, the sucking-dripping way possesses a few inescapable shortcomings, which are not beneficial to accurately test the electrical signal. These shortcomings mostly include (1) The self-assemblied nanofibers cannot totally be transferred on the electrode surface to form a compact and uniform film due to the adhesion effect of PTCDIs nanofibers on sucking-dripping instruments. (2) Injecting process breaks primal PTCDIs nanofibers, which is difficult to keep initial nanofibers state. (3) Large area electrode fabrication is not to employ the sucking-dripping way, which leads in an increase in fabricating cost and raw materials waste.

To realize the electrochemical study of PTCDI nanofibers, here, we directly deposited PTCDI nanofibers onto ITO glass (2 × 1 cm) in a glass cell (2.1 × 1.1 × 6 cm) after their formation from in situ self-assembly under V_{good}:V_{poor} = 1:4, as shown in Figure 6. The results of their surface morphologies via SEM measurement are shown in SI Figure S9. Such in situ deposition method can keep the initial state of the assembled PTCDI nanofibers, that is, not break their intact architectures, while mechanical damage is unavoidable for sucking-dripping moving. Also, it is quite effective with low energy consumption in contrast to conventional strategies. The layer by layer stacking state facilitates the construction of homogeneous and compact networks of PTCDI nanofibers with even distribution on the ITO glass substrates. Indeed, the fabrication of large area electrodes with full coverage of nanofibers has many benefits to overall device performance, but it should be noted that there are some twilight zones on the surface of some samples due to the soaking of ITO surfaces in the PTCDIs solutions before and during the deposition processes of assemblies. Moreover, the special functional carboxylate moieties of PTCDI 3 and PTCDI 4 at different pH values have, to a great degree, provided good adhesion of the as-prepared nanofibers on the ITO glass surface to form reliable interfacial contacts.[23−25] Certainly, the evident electric signal also could indicate the good interfacial adhesion with ITO electrode.

Electrochemistry of Nanofibril PTCDIs. A three-electrode system was employed to research the electrochemical properties of PTCDI nanofibers, and a 0.1 M Na_2SO_4 solution was used as the electrolyte. The CVs results are displayed in Figure 7. Every PTCDI nanofibril electrode displayed a reduction process from the CV curve due to the single-electron-transfer steps ascribing from one-electron reduction of the PTCDI skeleton to its monoanionic state, which was in accordance with the electrochemical properties of PTCDI monomer. However, nanofibril PTCDI exhibited a strong peak current compared with monomeric PTCDI in solution, which can be explained by well-ordered PTCDIs stacking on the conductive ITO surface. For PTCDI 1 and PTCDI 2 nanofibers, their electrochemical character was similar to that of the molecular solution at the negative range. And, PTCDI 1 nanofibers exhibited a strong oxidative peak due to the well-ordered stacking molecules and effective contact, which lead to the enhancement of the degree of oxidation for the adjacent EDOT species. Thus, PTCDI 1 nanofibers have shown enhanced peak current related to increased intra/intermolecular effective charge transport. Such results are good news for superior performance of nanofibril photoconductors and heterojunction optoelectronic devices. However, PTCDI 3 and PTCDI 4 nanofibers displayed distinct electrochemical curves exhibiting strong currents compared with their monomer electrochemistry. On one hand, the presence of triethylamine leads to the interfacial electron doping from the amine in electrolyte solution, followed by efficient long-range electron transport through the $\pi-\pi$ stacking way. On the other hand, the strong chemical binding with amines for PTCDI 3 and PTCDI 4 also contributes to the large electrical modulation.[18] Furthermore, their dimeric states in solution lead to form the hydrogen-bonded network on the lateral direction. Moreover, the presence of large amounts of COOH units attaching on nanofibril skeletons can form strong electrical contact with the electrode, minimizing the energy consumption of the electron transport at the electrode−active-material interface.[18] It is a reasonable explanation that the COOH unit is defined as an anchoring group which makes the molecules sensitive to pH due to protonation and deprotona-

DOI: 10.1021/acs.langmuir.9b01943
Langmuir 2019, 35, 12009−12016

tion. Particularly, the ionic and coordination interactions of COOH groups are partially responsible for the binding to ITO glass electrode surfaces.[23−25] Thus, these studies will provide novel insights and deep understanding about the design and construction of PTCDIs-involved optoelectronic devices, especially nanostructural materials with D-A, n-p, and other hybrid molecular structures or bulk architectures.

CONCLUSIONS AND OUTLOOK

In sum, the physicochemical properties and solution-phase self-assembly behavior of symmetric PTCDIs were investigated via tunable molecular structures. The optical and electrochemical properties of PTCDIs both in molecular and assembly state were critically discussed. In addition, the developed in situ deposition method following the in situ interfacial self-assembly of PTCDIs at room temperature will provide the feasibility to fabricate large-area electrodes for electrochemical characterization of nanoscale assemblies, whether they are generated from p-type or n-type semiconductors, and to construct electronic devices.

Such uniform electrode surfaces with large surface area attributed to abundant porosity will be desirable candidates to overcome recent difficulties in maintaining PTCDI nanofibers as a good candidate for OPVs, OFETs, OLED, bio/chem-sensors, photo/photoelectronic-catalysis, and other electronic or optoelectronic devices. The even, porous, and fully coated nanofibril electrodes make good contact between PTCDI nanofibers and other possible semiconductor molecules, polymers, or nanoassemblies to form reliable heterojunctions which have been widely utilized in several fields for the above-mentioned electronic devices. For example, such PTCDIs nanofibers covered ITO glasses as photoelectrocatalytic electrodes will provide a much large surface for contact with active species in the solutions or gaseous atmospheres. When as chemosensors, the full-covered and porous membrane construction and long-range charge carrier transfer along the 1D nanofiber frameworks will help enhance the sensing sensitivity and selectivity to analytes. The solution-phase assembly and room temperature throughout the whole process also will promote the promising development of this research in the future.

ASSOCIATED CONTENT

Supporting Information

The Supporting Information is available free of charge on the ACS Publications website at DOI: 10.1021/acs.langmuir.9b01943.

Materials, synthesis of PTCDIs, characterizations, fabrication methods of 1D nanostructures, results of FT-IR, TGA, UV−vis absorption, solubility, CV measurement, and SEM images (PDF)

AUTHOR INFORMATION

Corresponding Authors

*(S.C.) Phone: +1 801-809-7987; fax: +1 801-581-4816; e-mail: shuai.chen@utah.edu.

*(L.Z.) E-mail: lzang@eng.utah.edu.

ORCID

Shuai Chen: 0000-0001-8566-601X

Notes

The authors declare no competing financial interest.

ACKNOWLEDGMENTS

We are grateful to the National Natural Science Foundation of China (No. 51603095), the Scholarship from China Scholarship Council (No. 201808360327), Natural Science Foundation of Jiangxi Province (No. 20192BAB216012), Scientific Fund of Jiangxi Science & Technology Normal University (No. 2016QNBJRC003), Jiangxi Educational Committee for a Postgraduate Innovation Program Grant (No. YC2018-X29) for their financial support of this work.

REFERENCES

(1) Liu, X. P.; Kong, F. T.; Guo, F. L.; Cheng, T.; Chen, W. C.; Yu, T.; Chen, J.; Tan, Z. A.; Dai, S. Y. Influence of π-linker on Triphenylamine-Based Hole Transporting Materials in Perovskite Solar Cells. *Dyes Pigm.* **2017**, *139*, 129−135.

(2) Kini, G. P.; Oh, S.; Abbas, Z.; Rasool, S.; Jahandar, M.; Song, C. E.; Lee, S. K.; Shin, W. S.; So, W.-W.; Lee, J.-C. Effects on Photovoltaic Performance of Dialkyloxy-Benzothiadiazole Copolymers by Varying The Thienoacene Donor. *ACS Appl. Mater. Interfaces* **2017**, *9*, 12617−12628.

(3) Huang, Y. L.; Huang, W.; Yang, J. W.; Ma, J.; Chen, M. Y.; Zhu, H. Y.; Wang, W. Z. The Synthesis, Characterization and Flexible OFET Application of Three (Z)-1,2-bis(4-(tert-butyl)-phenyl)ethane Based Copolymers. *Polym. Chem.* **2016**, *7*, 538−545.

(4) Yi, W. J.; Zhao, S.; Sun, H. L.; Kan, Y. H.; Shi, J. W.; Wan, S. S.; Li, C. L.; Wang, H. Isomers of Organic Semiconductors Based on Dithienothiophenes: The Effect of Sulphur Atoms Positions on The Intermolecular Interactions and Field-Effect Performances. *J. Mater. Chem. C* **2015**, *3*, 10856−10861.

(5) Kim, J. S.; Kim, B.-M.; Kim, U.-Y.; Shin, H.; Nam, J. S.; Roh, D.-H.; Park, J.-H.; Kwon, T.-H. Molecular Engineering for Enhanced Charge Transfer in Thin-Film Photoanode. *ACS Appl. Mater. Interfaces* **2017**, *9*, 34812−34820.

(6) Xue, Y.; Xue, Z. X.; Zhang, W. W.; Zhang, W. N.; Chen, S.; Lin, K. W.; Xu, J. K. Enhanced Electrochromic Performances of Polythieno[3,2-b]thiophene with Multicolor Conversion via Embedding EDOT Segment. *Polymer* **2018**, *159*, 150−156.

(7) Yoon, G. B.; Kwon, H.-Y.; Jung, S.-H.; Lee, J.-K.; Lee, J. Effect of Donor Building Blocks on The Charge-Transfer Characteristics of Diketopyrrolopyrrole-Based Donor-Acceptor-Type Semiconducting Copolymers. *ACS Appl. Mater. Interfaces* **2017**, *9*, 39502−39510.

(8) Liu, J.; Jia, Y. H.; Jiang, Q. L.; Jiang, F. X.; Li, C. C.; Wang, X. D.; Liu, P.; Liu, P. P.; Hu, F.; Du, Y. K.; Xu, J. K. Highly Conductive Hydrogel Polymer Fibers toward Promising Wearable Thermoelectric Energy Harvesting. *ACS Appl. Mater. Interfaces* **2018**, *10*, 44033−44040.

(9) Uemura, T.; Rolin, C.; Ke, T.-H.; Fesenko, P.; Genoe, J.; Heremans, P.; Takeya, J. On the Extraction of Charge Carrier Mobility in High-Mobility Organic Transistors. *Adv. Mater.* **2016**, *28*, 151−155.

(10) Chen, S.; Slattum, P. M.; Wang, C. Y.; Zang, L. Self-Assembly of Perylene Imide Molecules into 1D Nanostructures: Methods, Morphologies, and Applications. *Chem. Rev.* **2015**, *115*, 11967−11998.

(11) Ding, C. M.; Shi, J. Y.; Wang, Z. L.; Li, C. Photoelectrocatalytic Water Splitting: Significance of Cocatalysts, Electrolyte and Interfaces. *ACS Catal.* **2017**, *7*, 675−688.

(12) Zeng, L.; Liu, T.; He, C.; Shi, D. Y.; Zhang, F. L.; Duan, C. Y. Organized Aggregation Makes Insoluble Perylene Diimide Efficient for The Reduction of Aryl Halides via Consecutive Visible Light-Induced Electron Transfer Processes. *J. Am. Chem. Soc.* **2016**, *138*, 3958−3961.

(13) Singh, R.; Shivanna, R.; Iosifidis, A.; Butt, H.-J.; Floudas, G.; Narayan, K. S.; Keivanidis, P. E. Charge versus Energy Transfer Effects in High-Performance Perylene Diimide Photovoltaic Blend Films. *ACS Appl. Mater. Interfaces* **2015**, *7*, 24876−24886.

DOI: 10.1021/acs.langmuir.9b01943
Langmuir 2019, 35, 12009−12016

(14) Zang, L. Interfacial Donor-Acceptor Engineering of Nanofiber Materials to Achieve Photoconductivity and Applications. *Acc. Chem. Res.* **2015**, *48*, 2705−2714.
(15) Li, D. W.; Liang, K.; Chen, W. L.; Li, C. M.; Zhao, D. Y.; Kong, B. Liquid-Solid Interfacial Assemblies of Soft Materials for Functional Freestanding Layered Membrane-Based Devices toward Electrochemical Energy Systems. *Adv. Energy Mater.* **2019**, *9*, 1804005−1804033.
(16) Wu, N.; Wang, C.; Slattum, P. M.; Zhang, Y. Q.; Yang, X. M.; Zang, L. Persistent Photoconductivity in Perylene Diimide Nanofiber Materials. *ACS Energy Lett.* **2016**, *1*, 906−912.
(17) Ramos, B.; Lopes, M.; Buso, D.; Ternisien, M. Performance Enhancement in N-channel Organic Field-effect Transistors Using Ferroelectric Material as A Gate Dielectric. *IEEE Trans. Nanotechnol.* **2017**, *16*, 773−777.
(18) Datar, A.; Balakrishnan, K.; Zang, L. One-Dimensional Self-Assembly of A Water Soluble Perylene Diimide Molecule by pH Triggered Hydrogelation. *Chem. Commun.* **2013**, *49*, 6894−6896.
(19) Li, Y. B.; Zhu, L.; Cheng, L. X.; Liu, C. H.; Liu, W.; Fan, Y. L.; Li, X.; Fan, X. L. pH-Induced Structural Transformation of *N*, *N*'-diaspartic acid-3, 4, 9, 10-tetracarboxylic Diimide as Observed by Scanning Probe Microscopy. *Surf. Interface Anal.* **2016**, *48*, 1002−1006.
(20) El-Khouly, M. E.; El-Refaey, A.; Shaban, Y. S.; El-Kemary, M. Optical Properties and Structural Morphology of One-Dimensional Perylenediimide Derivatives. *J. Lumin.* **2018**, *196*, 455−461.
(21) Tabacchi, G.; Calzaferri, G.; Fois, E. One-dimensional Self-assembly of Perylene-diimide Dyes by Unidirectional Transit of Zeolite Channel Openings. *Chem. Commun.* **2016**, *52*, 11195−11195.
(22) Zou, L.; You, A.; Song, J. G.; Li, X. Z.; Bouvet, M.; Sui, W. P.; Chen, Y. L. Cation-Induced Self-Assembly of An Amphiphilic Perylene Diimide Derivative in Solution and Langmuir-Blodgett Films. *Colloids Surf., A* **2015**, *465*, 39−46.
(23) Chen, F.; Li, X. L.; Hihath, J.; Huang, Z. F.; Tao, N. J. Effect of Anchoring Groups on Single-Molecule Conductance: Comparative Study of Thiol-, Amine-, and Carboxylic-Acid-Terminated Molecules. *J. Am. Chem. Soc.* **2006**, *128*, 15874−15881.
(24) Zhang, Z. J.; Lmae, T. Hydrogen-Bonding Stabilized Self-Assembled Monolayer Film of a Functionalized Diacid, Protoporphyrin IX Zinc(II), onto a Gold Surface. *Nano Lett.* **2001**, *1*, 241−243.
(25) Paik, W.-K.; Han, S.; Shin, W.; Kim, Y. Adsorption of Carboxylic Acids on Gold by Anodic Reaction. *Langmuir* **2003**, *19*, 4211−4216.

DOI: 10.1021/acs.langmuir.9b01943
Langmuir 2019, 35, 12009−12016